Atlantic Journal of Life Sciences
Volume 2026, Article ID 81, Pages 12
https://doi.org/10.71005/e1prqf61

Original Article

Integrated *in vitro*, *in vivo*, and in silico evaluation of antidiabetic and anti-inflammatory activities of *Melia azedarach* stem bark extract

Muhammad Shahab[1], Shahab Ud Din[1], Irfan Ullah[1], Ali Shan[1], Adnan Gul[1], Bushra Haider[1], Muhammad Tauqeer[2], Adil Sher[1], Gauhar Rehman[1]

[1]*Department of Zoology, Abdul Wali Khan University Mardan, 23200, Pakistan*| [2]*Department of Botany, Abdul Wali Khan University Mardan, 23200, Pakistan*

Correspondence shoud be addressed to Adil Sher; adilsher@awkum.edu.pk and Gauhar Rehman; gauhar@awkum.edu.pk

Received 31 Julay 2026; Revised 1 Augst 2026; Accepted 3 October 2026 ; Published 14 November 2026

KEYWORDS

Diabetes mellitus,
α-glucosidase,
α-amylase,
anti-inflammatory,
anti-diabetic,
in silico

ABSTRACT

This study investigated the anti-inflammatory and anti-diabetic potential of Melia azedarach stem bark extract (MASBE) using integrated in vitro, in vivo, and in silico approaches. Anti-diabetic activity was assessed through yeast glucose uptake, glucose adsorption, α-amylase, and α-glucosidase inhibition assays, followed by evaluation in an alloxan-induced diabetic mouse model. Anti-inflammatory activity was evaluated by human red blood cell (HRBC) membrane stabilization, heat-induced hemolysis, protein denaturation assays, and an in vivo xylene-induced ear edema model in mice. Molecular docking investigated the interactions of major phytoconstituents with inflammatory targets (COX-1, COX-2, and 5-LOX) and the anti-diabetic target AMPK. The extract showed potent anti-diabetic effects, including maximum yeast glucose uptake (78.99%), α-amylase inhibition (76.72%), and α-glucosidase inhibition (74.53%), along with effective glucose adsorption. In diabetic mice, MASBE significantly reduced blood glucose levels and improved body weight and pancreatic and liver histology. MASBE exhibited significant dose-dependent anti-inflammatory activity, achieving maximum inhibition of 63.76% in HRBC membrane stabilization, 56.09% in heat-induced hemolysis, and 69.69% in protein denaturation assays, while markedly reducing xylene-induced ear edema in mice. Molecular docking revealed favorable binding affinities of α-linolenic acid, protocatechuic acid, and cyanidin-3-O-β-D-glucoside toward inflammatory and diabetic targets, with docking scores ranging from −3.72 to −6.85 kcal/mol, supported by key hydrogen-bond interactions. The combined experimental and computational findings demonstrate that MASBE possesses potent anti-inflammatory and anti-diabetic activities. These effects are likely mediated through multiple mechanisms involving inhibition of inflammatory mediators and modulation of glucose metabolism, highlighting M. azedarach stem bark as a promising natural source for the development of multifunctional therapeutic agents.

Copyright © 2026 Muhammad Shahab *et al*. is an open-access article distributed under the Creative Commons Attribution License, which permits use, distribution, and reproduction in any medium, provided the original work is properly cited.

1. Introduction

Diabetes mellitus (DM) is a metabolic disorder characterized by a high blood sugar level caused by a total or partial absence of insulin (Ukwuani & Igbokwu, 2015). Elevated blood glucose levels harm several physiological systems, such as the circulatory and neurological systems, and cause the body to produce inadequate insulin (Mariadoss *et al*., 2022). In 2021, approximately 537 million adults were living with diabetes, representing about 10.5% of the global adult population, while diabetes-related healthcare expenditure reached nearly USD 966 billion. DM disrupts carbohydrate, lipid, and lipoprotein metabolism, leading to persistent hyperglycemia and contributing to metabolic and vascular complications, including atherosclerosis, hypertension, dyslipidemia, and abnormal insulin regulation (Zaharia *et al*., 2019). Numerous studies indicate a strong correlation between oxidative stress and the prevalence of T2DM (Rehman & Akash, 2017). Although synthetic α-amylase and α-glucosidase inhibitors, such as miglitol and acarbose, are effective in controlling postprandial blood glucose levels, their use may be associated with gastrointestinal adverse effects, including diarrhea, nausea, vomiting, and abdominal bloating (Padhi *et al*., 2020). Therefore, plant-derived extracts with glucose-lowering activity and potentially fewer adverse effects have gained considerable attention as alternative or complementary approaches for diabetes management. Several bioactive phytochemicals obtained from medicinal plants have also been investigated as complementary agents in the treatment of diabetes (Rehman *et al*., 2023). Inflammation represents the body's initial immunological response to infection, aiming to neutralize pathogens and initiate the repair of damaged tissues. This complex process is prevalent in various chronic diseases and allergic reactions (Gomes *et al*., 2008). Inflammation entails a series of molecular cascades and cellular activities, enhancing blood vessel permeability, promoting tissue dysfunction, and supporting tissue regeneration and restoration (Arulselvan *et al*., 2016). These chronic inflammatory disorders are a leading cause of mortality worldwide, contributing to over 50% of deaths. Risks associated with early development and long-term impacts persist throughout an individual's life (Singh *et al*., 2019). Initiated by pro-inflammatory cytokines, chemokines, adhesion molecules, and enzymes, prolonged inflammation can lead to numerous disorders, including cardiovascular diseases, cancer, diabetes, arthritis, Alzheimer's disease, pulmonary conditions, and autoimmune diseases (Sanada *et al*., 2018). The use of conventional drugs for managing inflammatory disorders may be associated with various adverse effects, highlighting the growing interest in natural products as potential safer alternatives for anti-inflammatory therapy.

Medicinal plants have received considerable attention from researchers worldwide as potential sources of safer and effective agents for diabetes management. Their therapeutic potential is largely attributed to diverse bioactive compounds that can exert significant pharmacological effects (Abid *et al*., 2022). In recent years, plant-derived medicines have gained increasing importance in the treatment of various diseases, reflecting a growing interest in their therapeutic applications compared with earlier periods. The Meliaceae family is rich in bioactive phytochemicals and polyphenolic compounds with reported antibacterial, antioxidant, antimicrobial, and anticancer activities (Malar *et al*., 2020). In Ayurvedic medicine, *Melia azedarach* has traditionally been employed for managing diverse health conditions, including respiratory ailments, inflammation, headaches, gastrointestinal disorders, diabetes, poisoning, and malaria

(Meena *et al*., 2026). *Melia azedarach*, commonly known as the chinaberry tree, is a deciduous member of the Meliaceae family. It is native to parts of Asia and Australia and has become widely established in warm-temperate regions worldwide (M'rabet *et al*., 2017). *Melia azedarach* has attracted interest as a potential natural biocontrol resource. Its leaves, fruits, and bark contain diverse bioactive constituents, including triterpenoids, limonoids, flavonoids, alkaloids, tannins, and phenolic compounds, contributing to its broad range of biological activities (El-Moaty *et al*., 2026). Historically, every part of this tree has been used as a home remedy for conventional treatment against different human diseases such as inflammation, leprosy, and cardiac disorders (Seifu *et al*., 2017). The root of *M. azedarach* Linn. is highly beneficial and effective in curing polyuria, polydipsia, Cancer, and diabetes mellitus (Huang *et al*., 2026; Nargund *et al*., 2018).

The present study aimed to comprehensively evaluate the anti-inflammatory and antidiabetic potential of *Melia azedarach* stem bark ethanolic extract (MASBE) using an integrated *in vitro*, *in vivo*, and *in silico* approach. *In vitro* anti-inflammatory activity was assessed using human red blood cell (HRBC) membrane stabilization, heat-induced hemolysis, and protein denaturation assays. The *in vitro* antidiabetic potential of MASBE was evaluated through yeast glucose uptake, glucose adsorption, and α-amylase and α-glucosidase inhibition assays. *In vivo* anti-inflammatory activity was investigated using the xylene-induced ear edema model, while antidiabetic effects were evaluated in alloxan-induced diabetic mice treated with different doses of MASBE. Furthermore, molecular docking was performed to evaluate interactions between selected bioactive phytoconstituents and key protein targets involved in inflammation and glucose metabolism, thereby providing mechanistic insights into the pharmacological activities of MASBE.

2. Materials and Methods

2.1 Materials and reagents

All chemicals and reagents used in this study were of analytical grade and were purchased from Sigma-Aldrich (St. Louis, MO, USA). These included ethanol, phosphate-buffered saline (PBS), sodium chloride (NaCl), chloroform, Xylene, formalin, alloxan monohydrate, baker's yeast, glucose, acarbose, metformin, and other reagents required for the experimental assays**.** The organic solvents and additional chemicals used in the study were obtained from Acarbose (Glucobay; Bayer) and metformin (D-Formin; Getz Pharma Pakistan (Pvt.) Ltd.) were used as standard antidiabetic drugs, while diclofenac sodium (Panslay; Getz Pharma Pakistan (Pvt.) Ltd.) was used as the standard anti-inflammatory drug. Blood glucose levels were measured using an Accu-Chek Active Glucometer (Roche Diagnostics, Germany)**.**

2.2 Study area and plant collection

The stem bark of *Melia azedarach* was collected from Shah Mansoor, District Swabi, Pakistan, after approval of the study by the Bioethics Committee of the Faculty of Biological Sciences, Abdul Wali Khan University Mardan. The collected plant material was taxonomically authenticated by Dr. Guljan, Department of Botany, Abdul Wali Khan University Mardan, Pakistan. A voucher specimen was prepared and deposited in the departmental herbarium under Voucher No. **Bot.202531** for future reference. To remove surface dust and contaminants, the collected stem bark was gently washed with running tap water. The gathered stem bark of the *Melia azedarach* plant was kept at room temperature and shade-dried for approximately three weeks. For future use, the stem bark was ground into powder after shade drying.

2.3 Plant extract preparation

The powdered stem bark (25 g) of Melia azedarach was mixed with 250 mL of absolute ethanol in a beaker. The beaker was covered with aluminum foil and placed in a shaker incubator at 45 °C for 72 h (kumar Bargah, 2015). After extraction, the mixture was filtered, and the residue was re-extracted twice with fresh ethanol to ensure efficient recovery of soluble phytochemicals. The solvent was removed using a rotary evaporator at 40 °C to obtain the crude ethanolic extract. The dried extract was stored in airtight containers at 4 °C until further use (Gomathi *et al*., 2015).

2.4 In vitro antidiabetic activities

2.4.1 Yeast glucose uptake assay

The in vitro antidiabetic activity was evaluated using the yeast glucose uptake assay. During the test, a slightly modified version of the (Sher *et al*., 2025) approach was employed to absorb glucose utilizing yeast cells. Commercial baker's yeast was dissolved in distilled water and allowed to stand at room temperature (27 °C) for the whole night. The next morning, the suspension of commercial baker's yeast cells was centrifuged for 5 minutes at 4200 rpm. The mixture of commercial baker's yeast cells was centrifuged repeatedly by the addition of distilled water to the pellet until a clear supernatant was formed. After centrifugation, 10% (v/v) suspensions of yeast cells were made by dissolving 1 mL of pure yeast in 9 mL of distilled water. 1 mL of a glucose solution (5mM) was mixed with various amounts of plant extracts (from 5 to 70µg/mL). At 37 °C, the solutions were incubated for 10 minutes. After incubation, mixtures were given a 100µl yeast suspension and vortexed, and then incubated at 37 °C for 60 minutes. The tubes were centrifuged for 10 minutes at 3800 rpm after incubation. Using a spectrophotometer set at 520 nm, the concentration of glucose in the supernatant solution was measured. Glucophage was used as a standard drug. At the same wavelength, the corresponding control's absorbance was similarly measured. By using the given formula, the percent increase in glucose uptake was determined

$$\text{Glucose uptake (\%)} = \frac{(\text{Control absorbance} - \text{sample absorbance})}{\text{Control absorbance}} \times 100$$

2.4.2 Glucose adsorption assay

The glucose adsorption capability of MASBE was evaluated by using a significantly modified procedure of (Rehman *et al*., 2023). 0.2 g of MASBE was poured into 100 mL glucose solution of five different concentrations (5–30mM). All mixtures were vortexed and stirred, incubated at room temperature for 6 h in a shaker water bath. After incubation, the mixture was centrifuged at 4800 rpm for 20 minutes. The amount of glucose was then measured by an Accu-Chek Active Glucometer (Roche Diagnostics, Germany). The formula was given below to calculate the quantity of bound glucose

$$\text{Bounded Glucose} = \frac{R1 - R2}{\text{Sample weight}} \times \text{volume of sample}$$

S1: Indicate the glucose concentration of the original solution

S6: Indicate the glucose concentration after 6 hours.

2.4.3 α-Amylase activity

The α-amylase inhibitory activity of the extract and standard drug (acarbose) was evaluated using the methods described in (Joshi *et al*., 2026; McCue & Shetty, 2004) with minor modifications. Various concentrations of the extract and standard drug (acarbose) (5–70 µg/mL) were prepared, and 250 µL of 0.02 M sodium phosphate buffer (pH 6.9) containing α-amylase (0.5 mg/mL) was added to each tube. The reaction mixtures were pre-incubated at 25 °C for 10 min. Next, 500 µL of a 1% starch solution prepared in 0.02 M sodium phosphate buffer (pH 6.9) was added, and the mixture was incubated at 30 °C for 15 min. The reaction was terminated by adding 0.05 mL of dinitrosalicylic acid reagent, followed by heating in a boiling water bath for 5 min. Absorbance was measured at 542 nm using a spectrophotometer. A control was prepared following the same procedure, with distilled water used instead of the extract. The α-amylase inhibitory activity was expressed as percentage inhibition and calculated using the standard formula given below:

$$\text{Inhibition percentage} = \frac{(\text{Control absorbance} - \text{Treated absorbance})}{\text{Control absorbance}} \times 100$$

2.4.4 α-Glucosidase activity

The effect of the plant extracts and Standard (acarbose) on α-glucosidase activity was determined according to the method described by (Sher *et al*., 2025), with a little modification. The substrate solution p-nitrophenyl glucopyranoside (pNPG) was prepared in 20 mM phosphate buffer at pH 6.9. 100 μL of α-glucosidase (1.0 U/mL) was pre-incubated with different concentrations of the extracts and the standard drug (acarbose) (5µg/mL to 70µg/mL) for 15 min. Then, 50 μL of 3.0 mM pNPG as a substrate dissolved in 20 mM phosphate buffer (pH 6.7) was added to start the reaction. The reaction mixture was incubated at 30 °C for 25 min and stopped by adding 2 mL of 0.1 M Na_2CO_3. The α-glucosidase activity was determined by measuring the yellow-colored paranitrophenol released

from pNPG at 405 nm. The results were expressed as inhibition percentage using the following formula.

$$\text{Inhibition percentage} = \frac{(\text{Control absorbance} - \text{Treated absorbance})}{\text{Control absorbance}} \times 100$$

2.5 In vitro anti-inflammatory activities

Anti-inflammatory activities of *Melia azedarach* stem bark extract (MASBE) were determined by *in vitro* methods such as HRBC membrane stabilization assay, Heat-induced hemolysis assay, and Egg Albumin protein denaturation assay.

2.5.1 HRBC membrane stabilization assay

The anti-inflammatory activity of *Melia azedarach* stem bark extract was assessed by the membrane stabilization assay with slight changes as described by (Sher, Zaib, *et al*., 2026). To prepare the red blood cell suspension, 5 mL of blood was obtained from a healthy individual in an EDTA tube who had not used anti-inflammatory medications for several days before the experiment. After that, the blood was centrifuged for 30 minutes at room temperature at 3000 rpm, and the normal saline 0.9% (w/v) was used to wash the red blood cells and remove the supernatant till the supernatant turned out to be clear. RBC suspension 10 % (v/v) was prepared with normal saline. The reaction mixture, with a volume of 2 mL, having 0.5 mL phosphate-buffered saline, pH 7.4, 1 mL hypo saline (0.25% w/v), 0.25 mL human red blood cell suspension, and 0.15 mL MASBE solution with varying concentrations 5, 10, 20, 30, and 40 µg/mL was prepared in normal saline and incubated at 37 °C for 30 min. The solution was centrifuged for 15 minutes at 3000 rpm and then the absorbance of supernatant by using a spectrophotometer at 560 nm. The following formula was used to calculate inhibition.

Inhibition (%) = (Control absorbance-Treated absorbance) ×100

(Control absorbance)

2.5.2 Heat-induced hemolysis assay

The anti-inflammatory potential of MASBE on heat-induced hemolysis of HRBC was assessed with slight changes as described by (Sher, Sohail, *et al*., 2026b). The collection of blood and preparation were discussed in the earlier assay. After that, a 1 mL reaction mixture was prepared by mixing 0.1 mL of 10 % suspension of the HRBC in Falcon tubes containing 0.15 mL of varying concentrations (5 – 40µg/mL) of MASBE dissolved in phosphate-buffered saline, pH 7.4, and the mixtures were incubated for 30 minutes at 54 °C. After incubation, the mixtures were centrifuged for 5 min at 5400 rpm, and then the absorbance of the supernatants was measured with a spectrophotometer at 560 nm. In the control, the extract was replaced by distilled water, while diclofenac sodium (5-40µg/mL) was used as the standard drug. Inhibition was calculated using the following formula.

Inhibition (%) = (Control absorbance-Treated absorbance) ×100

(Control absorbance)

2.5.3 Inhibition of protein denaturation assay

The egg albumin denaturation experiment was proposed to assess the anti-inflammatory properties of MASBE with slight modification as described by (Taj *et al*., 2022). A 2ml reaction mixture was prepared to have 0.2 mL fresh egg albumin and 0.3 mL of different concentrations (20, 40, 60, 80, and 100µg/ml) of MASBE dissolved in PBS (PH 6.4). Similarly, Diclofenac sodium was used as a standard drug. In the control, 0.2 mL of fresh egg albumin was dissolved in 1.8 mL of PBS (PH 6.4). The reaction mixture was incubated at 37°C for 15 minutes, and then heated for 5 minutes at 72 °C. The absorbance of the mixture was observed after cooling using a spectrophotometer at 660 nm. The following formula is used to calculate the percent inhibition of protein denaturation.

Inhibition (%) = (Control absorbance-Treated absorbance) ×100

(Control absorbance)

2.6 In vivo antidiabetic evaluation

Male albino mice aged 4 weeks and weighing 27-30 g were obtained from the Veterinary Research Institute, Peshawar, Pakistan. The animals were maintained on a standard laboratory diet with free access to water under controlled environmental conditions, including a 12 h light/12 h dark cycle, 57–60% humidity, and 20–23 °C temperature. All experimental procedures were conducted in accordance with the guidelines of the National Research Council for the care and use of laboratory animals. Ethical approval was obtained from the Ethical Committee of the Department of Zoology, Abdul Wali Khan University Mardan (AWKUM), Pakistan, under Ref. No. AWKUM Zoo-2025-1302, prior to the commencement of the study. For assessment of body weight and blood glucose levels, the mice were fasted for 11–13 h, after which blood samples were collected from the tail vein and glucose levels were measured using an Accu-Chek Active Glucometer (Roche Diagnostics, Germany) on days 1, 5, 10, 15, 20, and 25, while body weight was recorded at 5-day intervals. Diabetes was induced in the designated groups by intraperitoneal administration of alloxan monohydrate (170 mg/kg body weight) following an overnight fast, whereas the control group received distilled water. Seventy-two hours after alloxan administration, blood glucose levels were measured to confirm diabetes, and mice with glucose levels >280 mg/dL were considered diabetic and included in the subsequent *in vivo* experiments.

2.6.1 Experimental design

For the *in vivo* study, the mice were randomly divided into six groups, with three mice in each group (n = 3). Group I served as the normal control and received normal saline daily, while Group II comprised diabetic control mice treated with normal saline. Group III consisted of diabetic mice treated with metformin (1 mg/kg body weight) as the standard antidiabetic drug. Groups IV, V, and VI comprised diabetic mice treated with the plant extract at doses of 0.5, 1, and 2 mg/kg body weight, respectively.

2.6.2 Histopathological analysis of liver and pancreas

The pancreas and liver were removed, washed, preserved in 15% formalin, and processed using Histopathological techniques. The sample tissue was sliced into 5 to 7 µm thick slices, waxed, and stained with Hematoxylin and eosin before being analyzed through a microscope.

2.7 In vivo anti-inflammatory activity

Male Swiss albino mice, two weeks old and weighing 27–30 g, were obtained from the Veterinary Research Institute (VRI), Peshawar, Pakistan, for the *in vivo* experiment. The animals were maintained at 23–25 °C, with 40–45% relative humidity and a 12 h light/12 h dark cycle, and were provided with a standard laboratory diet and free access to tap water. The mice were moderately fasted before each experiment to minimize the influence of food intake on treatment responses. The animals were randomly divided into four groups, with three mice in each group (n = 3). Group 1 (negative control) received a standard diet and normal saline without any treatment. Group 2 (positive control) was subjected to ear edema induction using xylene but received no treatment. Group 3 (standard treatment) consisted of mice with induced ear edema treated with diclofenac sodium (1 mg/kg body weight). Group 4 (experimental treatment) consisted of mice with induced ear edema treated with *Melia azedarach* stem bark extract (MASBE) at doses of 0.5, 1, and 2 mg/kg body weight. Ear edema was induced by applying two drops of xylene to both sides of the right ear. Ear thickness was measured using a screw gauge before xylene application and at 1, 4, 12, and 24 h after treatment with diclofenac sodium or different doses of MASBE. The percentage inhibition of ear edema was calculated using the formula provided below.

% inhibition of ear edema = (Thickness of control-Thickness of sample) ×100

(Thickness of Control)

2.7.1 Histopathology

For histopathological analysis, mouse Liver, Pancreases, and ear tissues were collected and kept in small vials containing 10% formalin solution. The samples were sent to Ali's lab in Islamabad to make slides. The slides were then examined under a microscope.

2.8 Docking studies

2.8.1 Preparation of protein structures

To ensure accurate outcomes in structure-based molecular modeling, the use of well-defined protein structures is essential. In this research, the protein model generated by AlphaFold 2 was utilized for virtual screening purposes. The MOE (Molecular Operating Environment 2016) software's structure preparation tool was employed for the refinement of the protein model (Naz *et al*., 2021). The 3D protonation process was conducted to introduce hydrogen atoms into the protein structure, followed by energy minimization using the default settings of the MOE software.

2.8.2 Preparation of ligands

The ligand molecules protocatechuic acid (CID: 72), cyanidin-3-*O*-β-D-glucoside (CID: 12303203), stigmasterol (CID: 5280794), and α-linolenic acid (CID: 5280934) were retrieved from the PubChem database (https://pubchem.ncbi.nlm.nih.gov/). All ligands were prepared in the Molecular Operating Environment (MOE) software by three-dimensional protonation using the MMFF94x force field, followed by energy minimization with an RMS gradient of 0.05 before molecular docking analysis (Haider *et al*., 2020).

2.8.3 Molecular docking

The 3D crystal structures of the target proteins, including AMPK (PDB ID: 4CFF), COX-1 (PDB ID: 6Y3C), COX-2 (PDB ID: 4E1G), and 5-LOX (PDB ID: 3V99), were retrieved from the Protein Data Bank (PDB) (Sher, Sohail, *et al*., 2026a). The protein structures were prepared by removing water molecules and co-crystallized ligands, followed by 3D protonation and energy minimization using the Molecular Operating Environment (MOE 2016) software (Ullah *et al*., 2023). The selected phytochemicals, including protocatechuic acid (CID: 72), cyanidin-3-O-β-D-glucoside (CID: 12303203), stigmasterol (CID: 5280794), and α-linolenic acid (CID: 5280934), were retrieved from the PubChem database and prepared using MOE with the MMFF94x force field, followed by energy minimization to an RMS gradient (Ajmal *et al*., 2024). Molecular docking was performed using the GBVI/WSA dG scoring function with a rigid receptor approach (Jereva *et al*., 2022; Molla *et al*., 2023). Five poses were generated for each ligand, and the top-ranked conformations were selected for interaction analysis. The docking protocol was further validated using AutoDock Vina, and the resulting protein–ligand interactions were analyzed and visualized using MOE and PyMOL (Sulimov *et al*., 2021).

2.9 Statistical analysis

All experiments were performed in triplicate, and the data are presented as the mean ± standard deviation (SD). Statistical analyses of both the *in vitro* and *in vivo* data were conducted using IBM SPSS Statistics version 22 (IBM Corp., Armonk, NY, USA). Differences among groups were analyzed using two-way analysis of variance (ANOVA), followed by the appropriate post hoc test where applicable. A P value of < 0.05 was considered statistically significant. Graphs and figures were generated using OriginPro 2026 (OriginLab Corporation, Northampton, MA, USA).

3. Results

3.1 In vitro antidiabetic activities

The *in vitro* antidiabetic activity of *Melia azedarach* stem bark extract was evaluated using yeast glucose uptake, glucose adsorption, α-amylase inhibition, and α-glucosidase inhibition assays.

3.1.1 Yeast glucose uptake assay

The effects of different doses of MASBE and the standard drug Glucophage were investigated in a 5mM solution of glucose using glucose absorption by yeast cell tests. At concentrations of 5, 10, 20, 30, 40, 50, 60, and 70µg/mL of MASBE, the average percentage of glucose uptake by yeast cells was 7.971 ± 0.058%, 17.841 ± 0.137%, 28.436 ± 0.221%, 41.306 ± 0.299%, 54.128 ± 0.248%, 66.669 ± 0.483%, 75.365 ± 0.546%, and 78.988 ± 0.572%. The percentage of standard medicine Glucophage was determined to be 15.059 ± 0.427%, 26.987 ± 0.210%, 38.306 ± 0.299%, 49.451 ± 0.373%, 64.409 ± 0.491%, 75.365 ± 0.546%, 79.713 ± 0.578%, and 85.510 ± 0.620% when given at the same concentration as crude extract. This result showing significant result (p-value < 0.05) indicated in Figure 1A.

3.1.2 Glucose adsorption assay

The adsorption of glucose by the MASBE at various concentrations of glucose of 5, 10, 15, 20, 25, and 30mM indicated in Figure 1B. The result of recent work investigated that the MASBE demonstrated a considerable capacity for glucose adsorption at all tested concentrations. MASBE showed 1.13 ± 0.21%, 1.77 ± 0.25%, 2.8 ± 0.27%, 4.63 ± 0.31%, 6.8 ± 0.2% and 8.6 ± 0.1% adsorption of glucose, respectively. The adsorptions of glucose by the test sample were directly proportional to the concentration of glucose. The adsorption of glucose rises with an increase in the amount of glucose. Therefore, at 5mM glucose concentration, the lowest adsorption were observed, and at 30mM, the greatest.

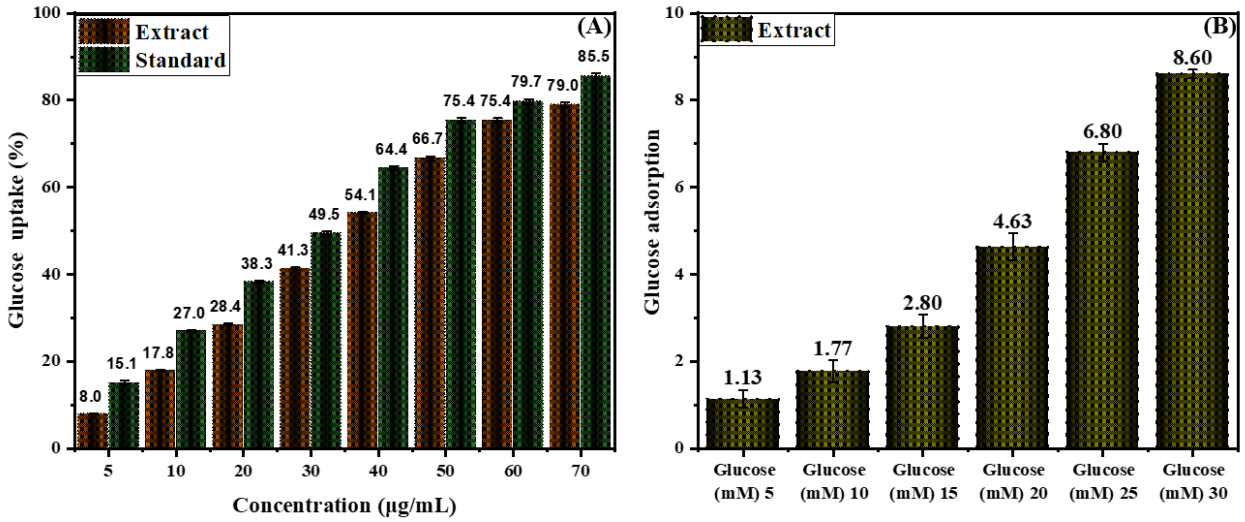


Figure1: (A) Glucose uptake by yeast cells using MASBE and **(B)** The ability of MASBE to bind glucose at different glucose concentrations

3.1.3 α-Amylase assay

The inhibitory potential of MASBE at (5, 10, 20, 30, 40, 50, 60, and 70 µg/mL) was evaluated, as revealed in Figure 2A. The inhibition percent of alpha-amylase of MASBE at 5, 10, 20, 30, 40, 50, 60 and 70 µg/mL were showed as 7.21 ± 0.7%, 23.19 ± 1.4%, 32.69 ± 0.9%, 50.26 ± 0.5%, 55.16 ± 1.3%, 62.67 ± 0.6%, 71.77± 1.6%, and 76.72 ± 1.3%, respectively. Whereas standard drug, showed % inhibition as 13.52 ± 0.8%, 35.26 ± 0.7%, 45.76 ± 0.5%, 55.17 ± 1.4%, 69.87 ± 0.9%, 74.72 ± 1.3%, 83.27± 1.4% and 89.76 ± 1.9% as a same concentration, respectively, *α*-Amylase activity of MASBE and standard drug (acarbose) showing significant result (p-value ≤ 0.001) showed in Figure 2A.

3.1.4 α-Glucosidase assay

The alpha-glucosidase enzyme, which is found on the mucosal brush border of the small intestine, is essential for digesting and breaking down complex carbs into smaller, more absorbable components. Inhibiting this enzyme can decrease glucose absorption, reduce high blood glucose levels, and perhaps halt diabetes development. At α-glucosidase concentrations of 5, 10, 20, 30, 40, 50, 60 and 70 µg/mL, the percentage inhibition by MASBE and standard drug (acarbose) was increased in a concentration-dependent manner the highest concentration of MASBE, and acarbose at a 70 µg/mL indicated the highest inhibition, 74.53±0.9%, and 80.33±2.2%. Thus, these outcomes exhibited MASBE, and standard have major potential in inhibiting α-glucosidase enzyme activity, as shown in (Figure 2B).

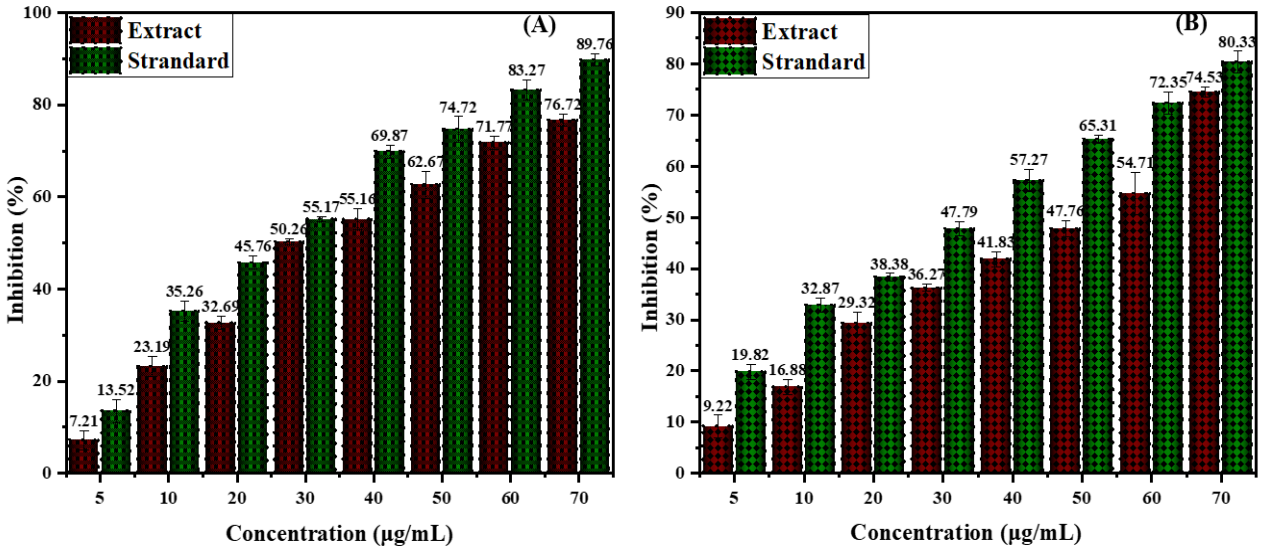


Figure 2: (A) Effect of stem bark crude extract of *M. azedarach* on alpha-amylase activity and **(B)** Effect of stem bark crude extract of *M. azedarach* on alpha-glucosidase activity

3.2 In vitro anti-inflammatory activities

3.2.1 Membrane stabilization assay

The membrane stabilization assay of *Melia azedarach* stem bark extract (MASBE) was evaluated on Human red blood cells (HRBCs), as shown in Figure 3A. The MASBE at concentrations of 5, 10, 20, 30, and 40 µg/mL showed inhibition of 8.025 ± 0.633%, 14.987 ± 0.633%, 33.076 ± 0.876%, 55.063 ± 0.633%, and 63.755 ± 0.684%, respectively. The maximum extract inhibition was noted at 40 µg/ml, while the standard drug, Diclofenac sodium, showed 69.219 ± 0.684% at a concentration of 40 µg/ml. This result is significant (p-value <0.005).

3.2.2 Heat-induced hemolysis assay

The results are shown in Figure 3B. MASBE inhibited heat-induced hemolysis by 9.491 ± 0.475%, 18.351 ± 0.686%, 35.807± 0.686%, 48.684 ± 0.475%, and 56.088 ± 0.686% at 5, 10, 20, 30, and 40µg/ml concentration, respectively. The effect was related to diclofenac sodium, which showed percentage inhibition of 15.00 ± 0.686%, 23.070 ± 0.945%, 41.404 ± 0.475%, 54.982 ± 0.686%, and 63.263 ± 0.590% at the same concentrations. This result is significant showing (p-value <0.001).

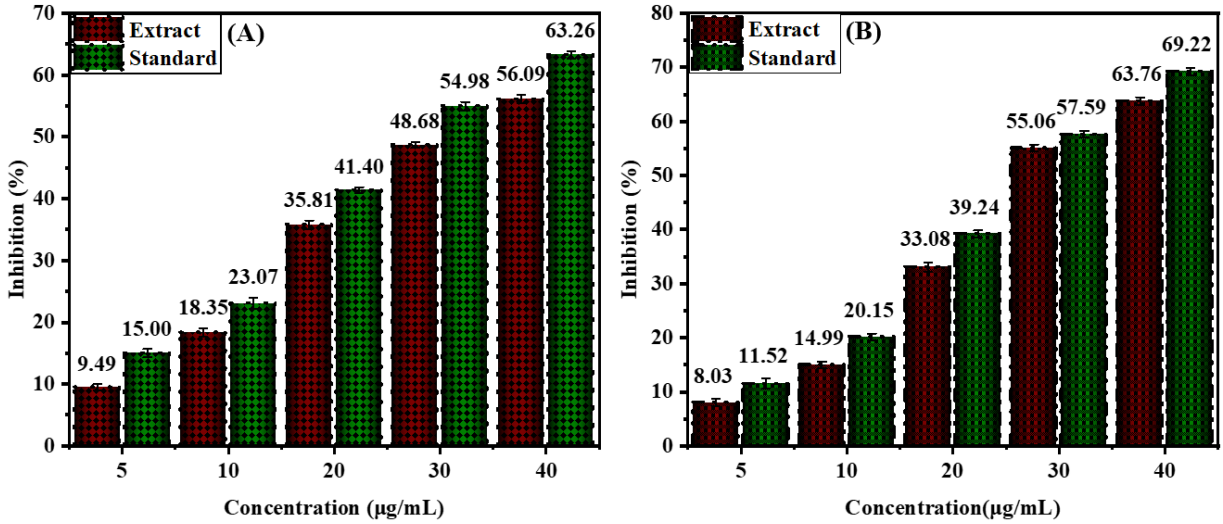


Figure 3. *In vitro* anti-inflammatory effect of MASBE evaluated by **(A)** HRBC membrane stabilization and **(B)** heat-induced hemolysis assay

3.2.3 Inhibition of protein denaturation assay

The inhibition rate of the protein denaturation assay for MASBE was increased with the increase of concentrations, as shown in Figure 4A. It has been noted that the maximum inhibition of MASBE was 69.687 ± 0.961% achieved at a concentration of 100µg/ml. The reference drug Diclofenac sodium showed the highest inhibition, 72.381 ± 0.422% at a concentration of 100 µg/ml. This result showed a significant p-value <0.0001.

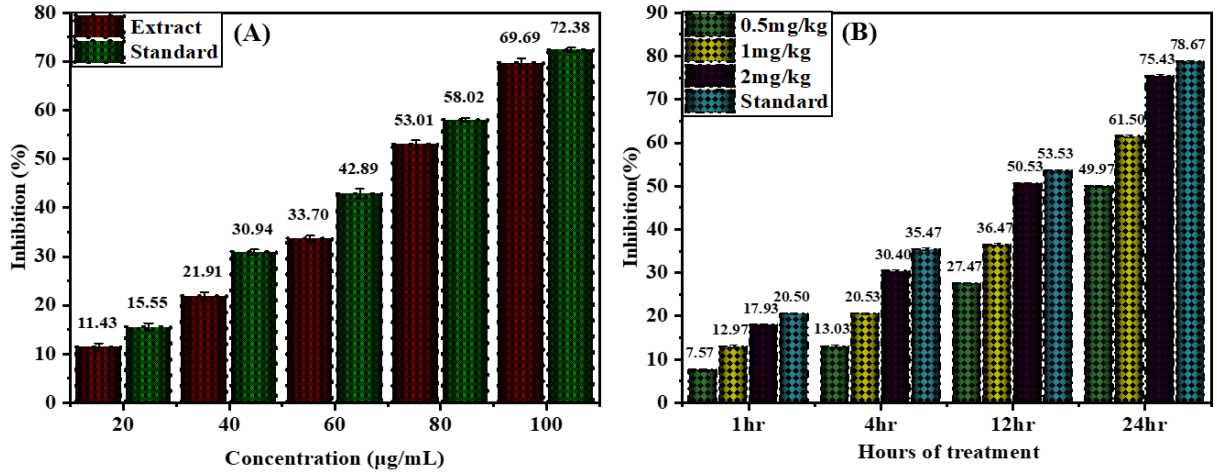


Figure 4. *In vitro* anti-inflammatory activity **(A)** protein denaturation assay and **(B)** *in vivo* anti-inflammatory effect of MASBE evaluated by Inhibition of xylene-induced

3.3 In vivo antidiabetic activity

3.3.1 Effect on blood glucose

Blood glucose levels rise after Alloxan was administered. Blood glucose level in experimental mice has been examined by treating diabetic mice with 0.5, 1, and 2 mg/kg body weight of MASBE for 25 days; it causes a significant decrease in hyperglycemia as indicated in Figure 5A. It is clear from Figure 5 that there was a significant increase in blood glucose levels (300.67 ± 6.506 to 334.33 ± 4.041 mg/dL) in the diabetic control group. The normal control group did not show a significant increase in blood glucose level (93 ± 8.888 to 107.33 ± 9.292 mg/dL). Groups of diabetic mice treated with MASBE at dosage of 0.5, 1, and 2mg/kg body weight, exhibited a substantial drop in blood glucose level (298.33 ± 4.163 to 201.67 ± 4.041 mg/dL, 285.67 ± 1.528 to 185.33 ± 0.577 mg/dL, 304.67 ± 13.317 to 156 ± 2 mg/dL), respectively. Mice with diabetes treated with 1mg/kg body weight of the standard drug Glucophage decreased the blood glucose level from 284.33 ± 3.055 to 140.67 ± 2.516.

3.3.2 Effect on body weight

During the experiment, the body weights of mice were assessed. The normal control group (Group I) showed a significant rise in value in just 25 days, rising from 24.73 ± 0.87g to 31.93 ± 0.51 g. Throughout the 25-day trial period, a gradual and noteworthy decrease from 25.33 ± 0.85g to 20.1 ± 1.1 g in body weight was noted in the Alloxan-induced diabetic mice (Group II). In contrast, the diabetic mice of group III, which was administered the standard drug Glucophage (1mg/kg body weight), experienced a rise in body weight from 25.63 ± 0.61g to 31.07 ± 0.85 g. A comparable pattern of activity was noted, whereby the effects of MASBE increased the body weight of diabetic mice of group IV, V and VI treated with varying doses (0.5, 1 and 2 mg/kg body weight) from 24.6 ± 0.6 to 29.27 ± 0.95 g, 24.7 ± 0.69 to 29.67 ± 0.95 g and 24.6 ± 0.46 to 30.33 ± 1.40 g, respectively, as illustrated in Figure 5B.

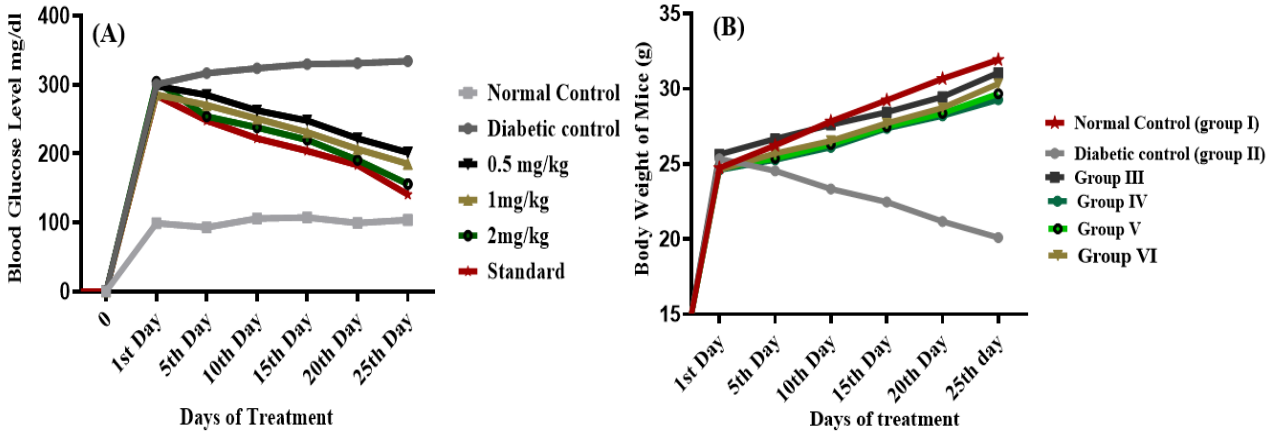


Figure 5: **(A)** Impact of stem bark crude extract of *M. azedarach* and Glucophage on blood glucose levels (mg/dL) in Alloxan induced diabetic mice. And **(B)** Impact of MASBE and Glucophage on body weight of mice.

3.3.3 Pancreatic histology

Microscopic analysis of the pancreas demonstrated that the normal control possessed a normal pancreas with uniformly distributed, tightly arranged β-cells (Figure 6A). Figure 6B illustrates that the pancreatic β-cells of mice treated with Alloxan were nearly total harm and may stop producing insulin. The endocrine and exocrine sections of the diabetic control group both showed pathological changes. The diabetic mice (Group III) that were administered with 1 mg/kg body weight of standard drug Glucophage showed the normal architecture of islets of the pancreas as seen in Figure 6C. Diabetic mice (Group IV) that received a dose of 0.5 mg/kg body weight of MASBE showed initial recovery of β-cells of the islets of the pancreas (Figure 6D). The islets of the pancreas in diabetic mice (Group V) were treated with 1 mg/kg body weight of MASBE (Figure 6E). From Figure 6F clear that diabetic mice (Group VI) treated with a dose of 2 mg/kg body weight of MASBE showed normal architecture and regeneration of normal β-cells shape of islets of the pancreas. The acinar cells had little degenerative change, and the pancreatic endocrine and exocrine portions could now be distinguished from one another, as shown in Figure 6F and 6C.

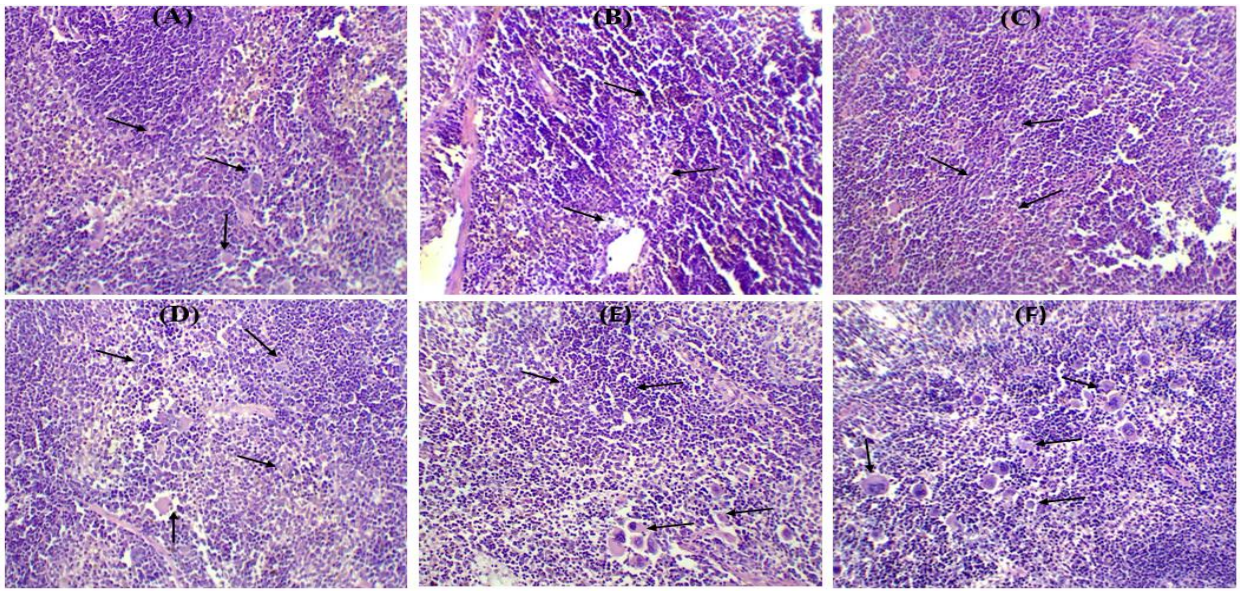


Figure 6: Histological study of the pancreas **(A)** Group I: the normal control, possessed a pancreas that was normally distributed and closely packed with β-cells **(B)** Group II: in the diabetic control group, pancreatic β-cells are nearly completely destroyed **(C)** Group III: treated with 1mg/kg b/w of standard drug Glucophage revealed normal-shaped Langerhans islets **(D)** Group IV: treated with 0.5mg/kg b/w of MASBE indicated β-cells in the pancreatic islets were starting to recover **(E)** Group V: treated with 1mg/kg b/w of MASBE; shown the islets of pancreas were partially recovered **(F)** Group VI: treated with 2mg/kg b/w of MASBE show normal architecture and regeneration of β-cells of pancreas.

3.3.4 Liver histology

The liver tissue of experimental mice was examined under a microscope to illustrate that MASBE decreases hepatocyte damage. The histology of the liver in the normal control group (Group I) exhibited a typical normal liver image (Figure 7A). Severe hepatic degeneration and death were observed in the hepatocytes of the diabetic control group (Group II) (Figure 7B). After receiving a dose of 1 mg/kg body weight of the standard drug Glucophage, the hepatocytes in the liver of diabetic mice (Group III) exhibited an identical and normal histological appearance as that of hepatocytes in the normal control group (Figure 7C). Figure 7D illustrated that the modifications in the size of the vacuoles of hepatocytes were observed in the liver of diabetic mice (Group IV) that received a dose of 0.5 mg/kg body weight of MASBE. The liver deterioration and hepatocyte destruction in diabetic mice (Group V) were considerably decreased when treated with a dose of 1 mg/kg body weight of MASBE (Figure 7E). Hepatocytes in the liver of diabetic mice (Group VI) treated with a dose of 2mg/kg body weight of MASBE present a normal structure and normal hepatocyte size (Figure 7F).

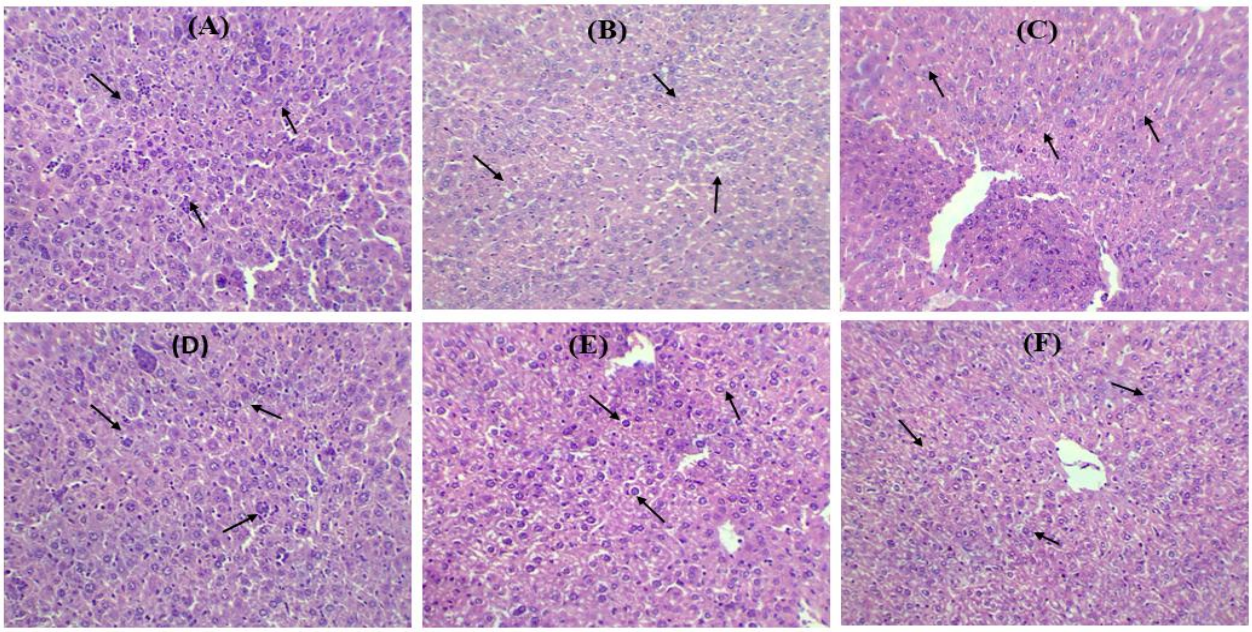


Figure 7: Liver histopathology, **(A)** Group I: normal control; normal liver shape **(B)**; diabetic control; shown significant hepatic deterioration and death **(C)** Group III: received 1 mg/kg b/w of the standard drug Glucophage; normal histological appearance of hepatocytes **(D)** Group IV: treated with 0.5 mg/kg b/w of MASBE; a slight reduction occurred in degeneration and necrosis of hepatocytes **(E)** Group V: treated with 1 mg/kg b/w of MASBE; considerable hepatocyte destruction occurred **(F)**; Group VI: treated with 2 mg/kg b/w of MASBE; normal regeneration of hepatocytes occurred.

3.4 Xylene-induced ear edema

The mean of xylene-induced ear edema of different groups of mice calculated at 1, 4, 12, and 24 hours is shown in Figure 8. The highest inhibition of MASBE at doses of 0.5, 1, and 2mg/kg showed 49.967 ± 0.451%, 61.5 ± 0.5%, and 75.433 ± 0.513% anti-inflammatory activity by reducing ear edema calculated at 24 hours, respectively. The effect of diclofenac sodium showed inhibition of ear edema calculated at 24 hours is 78.667 ± 0.577 at a dosage of 1mg/kg. This result showed a significant (p-value <0.0001), as shown in Figure 4.

3.4.1 Ear histology

Histological examination of the ears treated with xylene Figure 8. Showed a prominent increase in epidermis thickness and edema when compared to the control group. Either topical application of the MASBE (0.5, 1, and

2 mg/kg) or diclofenac sodium (1 mg/kg) was able to decrease inflammation, as shown in Figure 8.

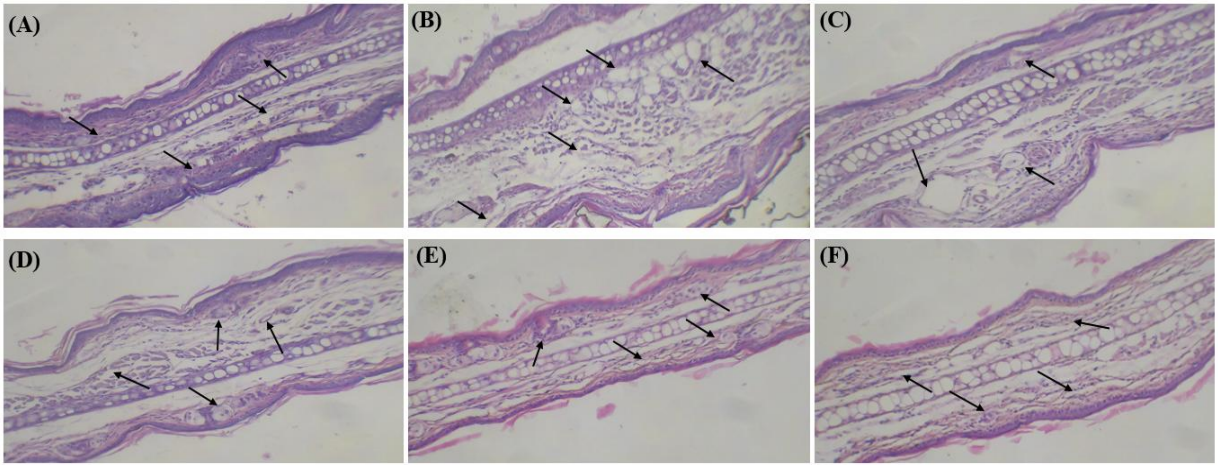


Figure 8: MASBE effects on xylene-induced ear edema. (**A**) Shows the negative control, (**B**) shows the positive control, while (**C, D, and E**) show the effect of MASBE at various concentrations, and (**F**) shows the effect of the standard drug diclofenac sodium.

3.5 In silico antidiabetic analysis

This study utilized molecular docking to investigate the interactions between 5′-adenosine monophosphate-activated protein kinase (AMPK) and the target compounds Protocatechuic acid and Cyanidin-3-O-β-D-glucoside. The active site residues were identified using MOE software, and docking scores were sorted for interaction analysis. Protocatechuic acid formed a hydrogen bond with GLU100, scoring -3.7184 kcal/mol, while Cyanidin-3-O-β-D-glucoside formed a hydrogen bond with GLU194 and an ionic bond with ARG188, scoring -5.6622 kcal/mol (Figures 9A, B). To validate these results, additional docking was conducted using AutoDock Vina, yielding comparable binding energies ranging from -3.2 to -5.8 kcal/mol. detailed interactions are summarized in **Table.1:**

Table 1: Binding energy scores and residue interactions of docked ligands.

Compound ID	Compound name	Docking score (S)	Receptor			Interaction	Distance	E (Kcal/mole)
CID_72	Protocatechuic acid	-3.7184	OE2	GLU	100	H-donor	3.17	-2.3
CID_12303203	Cyanidin-3-O-β-D-glucoside	-5.6622	OE1	GLU	194	H-donor	3.12	-2.4
			NH1	ARG	188	Ionic	3.24	-3.0

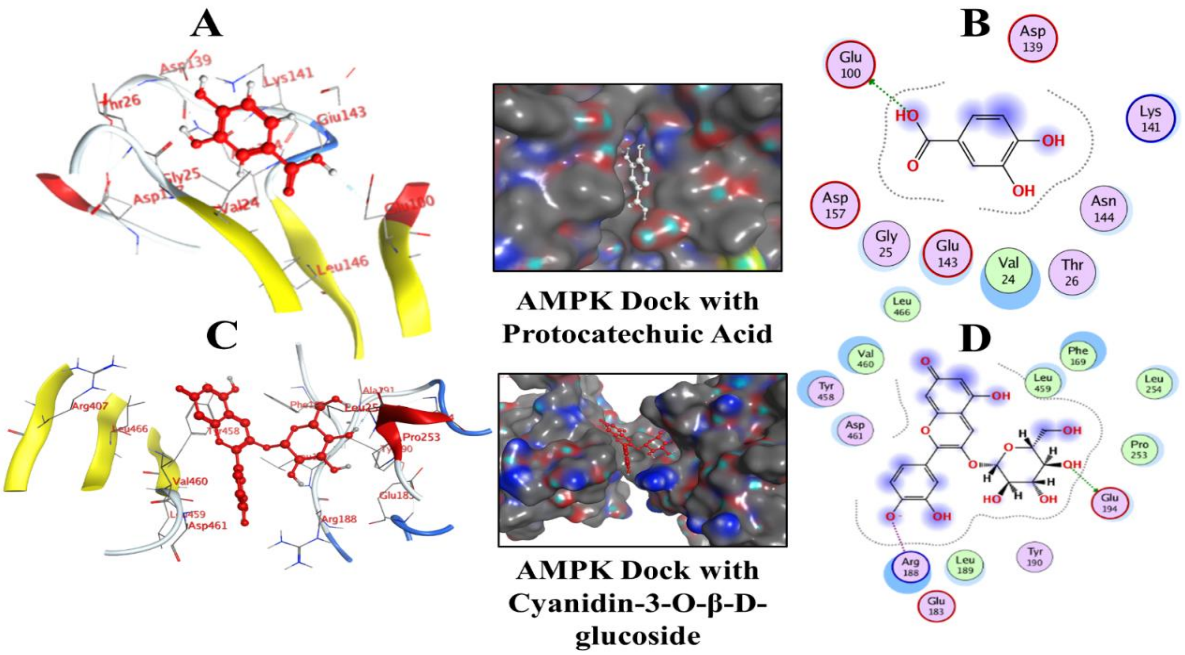


Figure 9: Molecular docking of the compounds Protocatechuic acid (**A, B**), and Cyanidin-3-O-β-D-glucoside (**C, D**) with the AMPK gene.

3.6 In silico anti-inflammatory analysis

In this study, molecular docking was employed to investigate the interactions of cyclooxygenase 1 (COX-1), cyclooxygenase 2 (COX-2), and 5-lipoxygenase (5-LOX) with the target compounds; α-Linolenic acid. The active site residues were identified using the site finder tool in MOE software. The docking scores of the compound α-Linolenic acid with COX1 exhibited three hydrogen bonds with ARG79 (H-donor), ARG79 (H-acceptor), and ARG79 (H-acceptor), achieving a docking score of -6.591 kcal/mol Figure 10 A, B. Compound α-Linolenic acid with COX2

displayed two hydrogen bonds with ASN39 (H-donor) and CYS41 (H-acceptor), resulting in a docking score of -6.845 kcal/mol Figure 10 C, D. Furthermore, the compound α-Linolenic acid with 5-LOX gene mediated one hydrogen bond donor (PRO152), yielding a docking score of -6.548 kcal/mol Figure 10 E, F. To improve docking success, the compounds identified by MOE were further docked with AutoDock Vina. The binding energies obtained from AutoDock were compared to the S scores from MOE, showing similar values ranging from -6.1 to -6.8 kcal/mol. The detailed binding interactions of 5′-adenosine monophosphate-activated protein kinase (AMPK), cyclooxygenase 1 (COX-1), cyclooxygenase 2 (COX-2), and 5-lipoxygenase (5-LOX) with the active site for the selected compounds are shown in Table 2.

Table 2: Predicted binding affinities and key residue interactions of docked compounds.

Compound ID	Compound name	Docking score (S)	Receptor			Interaction	Distance	E (Kcal/mole)
CID_5280794	Stigmasterol	-6.1372	OE1	GLU	194	H-donor	2.64	-1.6
CID_5280934	α-Linolenic acid	-6.5911	ONE	ARG	79	H-donor	2.70	-3.0
				ARG	79	H-acceptor	2.89	-3.9
			NH2	ARG	79	H-acceptor	2.94	-4.9
		-6.8455	OD1	ASN	39	H-donor	2.70	-5.4
			N	CYS	41	H-acceptor	3.27	-0.7
		-6.5487	O	PRO	152	H-donor	3.12	-2.6

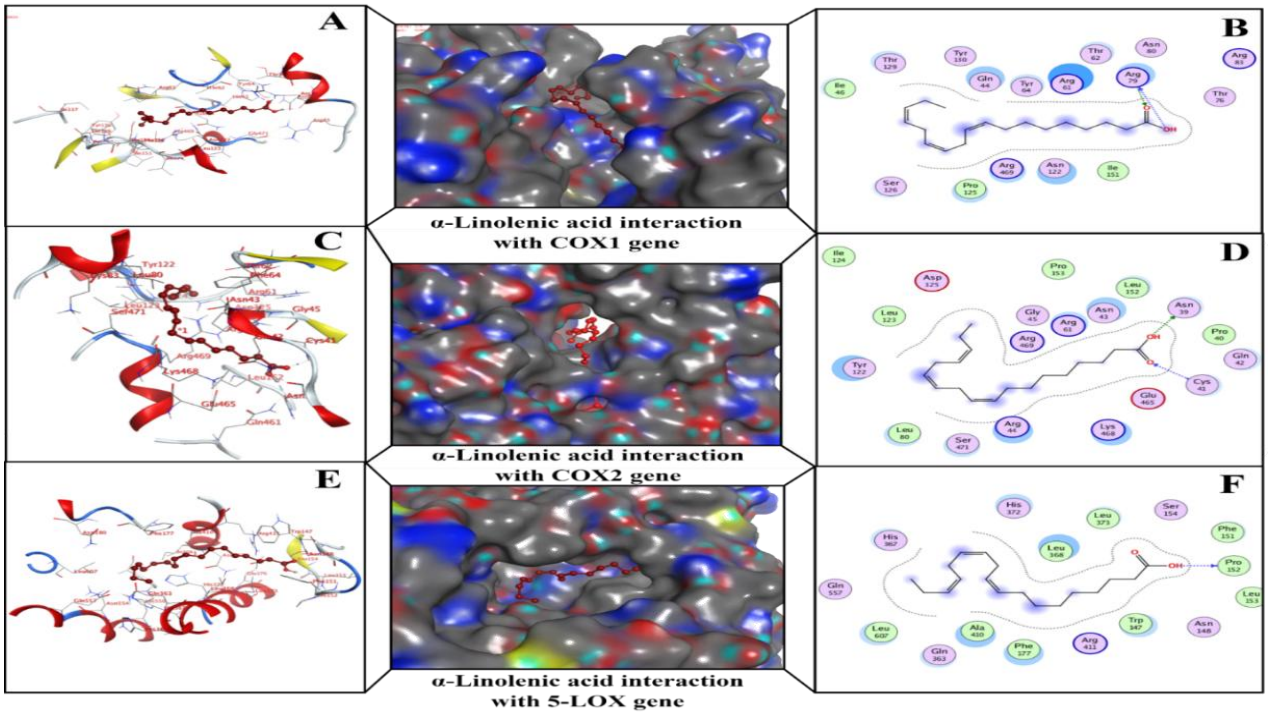


Figure 10. Molecular docking of the compound α-Linolenic acid with COX1 gene (**A, B**), COX2 gene (**C, D**), and 5-LOX gene (**E, F**).

4. Discussion

Diabetes is a global, severe, and rapidly developing disease characterized by inadequate insulin production and decreased tissue insulin susceptibility (Salehi *et al*., 2019). Oral hypoglycemic medications, including sulfonylureas, biguanides, and α-glucosidase inhibitors, thiazolidinediones, and non-sulfonylurea secretagogues, work to prevent diabetes by increasing insulin release from the islets of Langerhans. Insulin and synthetic oral hypoglycemic medications are crucial for managing diabetes, but they cannot fully prevent its progression due to their adverse effects (Kooti *et al*., 2015). Medicinal plants are now suggested for the therapy of several illnesses, including diabetes (Kumari *et al*., 2016). Numerous plants from various genera, such as Ficus, Artemisia, Solanum, Terminalia, and Euphorbia, exhibit anti-diabetic properties (Shinkafi *et al*., 2015). *Melia azedarach* Linn, also referred to as Indian lilac or Pride of India. It is mostly grown in the Himalayan regions of Pakistan, India, China, Burma, and Bangladesh. The medicinal use of this plant in Siddha, Unani, and Ayurveda is widely established. Stem bark possesses vermifuge, anti-periodic, astringent, bitter, and tonic properties. Several scholarly publications demonstrate that the *Melia azedarach* plant possesses numerous biological properties such as anticancer, antimalarial, analgesic, anti-inflammatory, anti-anthelmintic, anti-lithic, and diuretic effects (Khan *et al*., 2018).

In the present study, *Melia azedarach* stem bark ethanolic extract (MASBE) was comprehensively evaluated for its anti-diabetic and anti-inflammatory potential using integrated *in vitro*, in vivo, and in silico approaches. The anti-diabetic activity was investigated through yeast glucose uptake, glucose adsorption, α-amylase, and α-glucosidase inhibition assays, followed by evaluation in an Alloxan-induced diabetic mouse model. In addition, molecular docking studies were performed to

examine the interactions of major phytoconstituents with 5′-adenosine monophosphate-activated protein kinase (AMPK), a key regulator of glucose metabolism. The anti-inflammatory activity of MASBE was assessed using human red blood cell (HRBC) membrane stabilization, heat-induced hemolysis, and protein denaturation assays, followed by the xylene-induced ear edema model in mice. Furthermore, molecular docking was conducted against key inflammatory targets, including cyclooxygenase-1 (COX-1), cyclooxygenase-2 (COX-2), and 5-lipoxygenase (5-LOX), to elucidate the possible molecular mechanisms underlying its anti-inflammatory effects. The combined findings demonstrate that MASBE possesses significant anti-diabetic and anti-inflammatory activities, highlighting its potential as a promising natural therapeutic agent for the management of these metabolic and inflammatory disorders.

MASBE demonstrated significant antidiabetic activity in both the yeast glucose uptake and glucose adsorption assays. In the yeast glucose uptake assay, the extract significantly enhanced glucose uptake by yeast cells in a concentration-dependent manner over the tested concentration range (5–70 µg/mL) in a 5 mM glucose solution. The lowest glucose uptake (7.97 ± 0.06%) was observed at 5 µg/mL, while the highest uptake (78.99 ± 0.57%) was recorded at 70 µg/mL. Similarly, in the glucose adsorption assay, MASBE exhibited a concentration-dependent increase in glucose adsorption capacity at glucose concentrations ranging from 5 to 30 mM. The extract showed the lowest glucose adsorption activity (1.13 ± 0.21%) at 5 mM glucose and the highest activity (8.60 ± 0.10%) at 30 mM glucose. These findings indicate that MASBE effectively enhances glucose uptake and glucose adsorption, supporting its potential antidiabetic activity. In the α-amylase assay, inhibition increased from 7.21 ± 0.70% to 76.72 ± 1.30%, while the standard drug (acarbose) showed 13.52 ± 0.80% to 89.76 ± 1.90% inhibition over the same concentration range. Similarly, α-glucosidase inhibition by MASBE increased with concentration, reaching 74.53 ± 0.90% at 70 µg/mL, compared with 80.33 ± 2.20% for acarbose. These results indicate that MASBE possesses significant inhibitory activity against both carbohydrate-hydrolyzing enzymes ($P \leq 0.001$). Similarly, the current study shows correlation with the findings of research conducted by (Rehman *et al*., 2023).

Since ancient times, medicinal plants and plant-derived formulations have been widely used across various cultures to treat inflammatory disorders and related diseases. In this study, the anti-inflammatory activity of *Melia azedarach* stem bark extract (MASBE) was confirmed through membrane stabilization, heat-induced hemolysis, and protein denaturation assays, all of which showed dose-dependent effects. RBC and lysosomal membranes share similar structural characteristics. During inflammation, lysosomal membrane destabilization can promote the release of inflammatory mediators and hydrolytic enzymes, thereby contributing to tissue injury. Therefore, membrane stabilization may help prevent the release of these lysosomal components and subsequently reduce inflammatory responses (Oyeleke *et al*., 2018). In this study MASBE exhibited maximum membrane stabilization of 63.76% compared with 69.22% for diclofenac sodium, while heat-induced hemolysis was inhibited by 56.09% compared with 63.26% for the standard drug. Similar to our findings, previous studies have reported that plant extracts can protect erythrocyte membranes against heat-induced damage, indicating potential anti-inflammatory activity through membrane stabilization (Khan *et al*., 2022). These findings support the anti-inflammatory effects observed for *Melia azedarach* extracts in the present study. In the protein denaturation assay, MASBE achieved 69.69% inhibition, comparable to that of diclofenac sodium (72.38%). These anti-inflammatory effects may be attributed to the presence of flavonoids, phenolics, tannins, and other bioactive phytochemicals that stabilize cell membranes, inhibit protein denaturation, reduce oxidative stress, and suppress inflammatory mediators. Overall, the findings indicate that MASBE is a promising natural source of anti-inflammatory compounds.

The present study demonstrates that Alloxan administration increased blood glucose levels. Blood glucose levels were significantly increased in diabetic mice by the 25th day after alloxan injection, indicating persistent hyperglycemia in the diabetic control group. The normal control group did not show any significant increase. Groups treated with MASBE at doses of 0.5, 1 and 2 mg/kg body weight, exhibited significant decrease in blood glucose levels (298.33 ± 4.163 to 201.67 ± 4.041 mg/dL, 285.67 ± 1.528 to 185.33 ± 0.577 mg/dL, 304.67 ± 13.317 to 156 ± 2 mg/dL) ($p < 0.05$). These results were found to be similar to previous research carried out by (Rahman *et al*., 2023). The body weight of mice was measured, showing a significant increase in the normal control group (group I) over 25 days. The Alloxan-induced diabetic mice (group II) experienced a gradual decrease in body weight. MASBE effectively raised the body weight (24.6 ± 0.6 to 29.27 ± 0.95 g, 24.7 ± 0.69 to 29.67 ± 0.95 g, and 24.6 ± 0.46 to 30.33 ± 1.40 g) (p value < 0.05) of diabetic mice (Group IV, V, and VI) provided with different dosages (0.5, 1 and 2 mg/kg body weight). The result of this investigation supported the findings of (Mechchate *et al*., 2021). In the current study, in the histological analysis, the cells of the pancreas of the normal control were thoroughly and evenly distributed. The pancreas of untreated diabetic control groups contained highly distorted islet cells and acinar cells. Alloxan treatment caused nearly total harm to pancreatic cells in mice. The initial recovery of β-cells of pancreatic islets in diabetic mice was observed after treatment with a dose of 0.5 mg/kg body weight of MASBE. The islets were partially recovered in diabetic mice treated with a dose of 1 mg/kg body weight of MASBE. Diabetic mice cured with 2 mg/kg body weight of MASBE showed normal structure and restoration of normal β-cells shape. These results have a good and close connection with (Rehman *et al*., 2023). A histopathological study was performed to examine liver tissue in experimental mice to demonstrate that MASBE decreases cellular damage. The liver histology showed normal liver tissue in the normal control group. Significant liver necrosis and degradation were observed in the hepatocytes of the diabetic control group. The diabetic mice treated with 0.5 mg/kg body weight of MASBE showed visible hepatocytes in the liver. The mice with diabetes that received 1 mg/kg body weight of MASBE showed reduced liver deterioration and hepatocyte necrosis. The mice that were treated with 2 mg/kg body weight of MASBE showed a similar histological appearance of the liver as the normal control group. This result is similar to the study conducted to evaluate the anti-diabetic effects of bio-synthesized silver nanoparticles utilizing *P. spadiceum* extract (Sher, Zaib, *et al*., 2026). The *in vivo* anti-inflammatory activity of MASBE was evaluated using the xylene-induced ear edema model in mice. MASBE produced a dose-dependent reduction in ear edema, with inhibition ranging from 49.97% to 75.43% at doses of 0.5–2 mg/kg**,** respectively. The highest dose exhibited activity comparable to the standard drug, diclofenac sodium (78.7% inhibition), demonstrating the significant anti-inflammatory potential of MASBE. The In-silico study of anti-diabetic activity carried out on macromolecular targets involved in diabetes proposed that Protocatechuic Acid and Cyanidin-3-O-β-D-glucoside act through interaction with AMPK, for which the most capable calculated values were retrieved. The docking scores of Protocatechuic Acid and Cyanidin-3-O-β-D-glucoside are shown in Table 1**.** The docking study is consistent with the previous study, which identified a comparable pattern of interactions (Rauf *et al*., 2023). The computational studies of anti-inflammatory was carried out on various macromolecular targets involved in inflammation, suggesting that α-linolenic acid especially acts through the interaction with COX-1, COX-2, and 5-LOX, for which the most promising calculated binding values were retrieved. More specifically, the docking scores computed for α-linolenic acid are shown in Figures 6 a**nd 7**.

5. Conclusion

The present study demonstrates that *Melia azedarach* stem bark ethanolic extract (MASBE) possesses significant anti-diabetic and anti-inflammatory activities, as evidenced by comprehensive *in vitro*, in vivo, and *in silico* investigations. MASBE effectively enhanced glucose uptake and Glucose adsorption, inhibited α-amylase and α-glucosidase activities, reduced blood glucose levels, improved pancreatic and liver histology in diabetic mice, and exhibited marked anti-inflammatory effects through membrane stabilization, inhibition of protein denaturation and hemolysis, and inhibition of ear edema. Molecular docking further supported these biological activities by revealing favorable interactions between the major phytoconstituents and key protein targets involved in glucose metabolism and inflammatory pathways. The observed pharmacological effects are likely associated with the synergistic action of flavonoids, terpenoids, limonoids, and other bioactive constituents present in MASBE. Overall, these findings highlight *M. azedarach* stem bark as a promising natural source for the development of safer, multi-target therapeutic agents for the management of diabetes and inflammation. Further studies are recommended to isolate the active compounds, elucidate their molecular mechanisms, and evaluate their clinical potential.

Declarations

Ethics approval and consent to participate

Animal experiments were approved by the Ethics Committee of the Department of Zoology, Abdul Wali Khan University Mardan (approval reference reported in the manuscript: AWKUM Zoo-2025-1302). The manuscript also describes human blood collection for the HRBC assays; the authors must confirm the applicable human ethics approval and informed consent information before publication.

Consent for publication

not applicable

Availability of data and materials

Data availability is included in the paper

Competing interests

Authors declare no conflict of interest

Funding

not applicable

Authors' contributions

Authors to provide individual contributions and confirm approval of the final manuscript

Acknowledgments

not applicable

References

Abid, R., Islam, M., Saeed, H., Ahmad, A., Imtiaz, F., Yasmeen, A., & Rathore, H. A. (2022). Antihypertensive potential of Brassica rapa leaves: An in vitro and in silico approach. *Frontiers in Pharmacology*, *13*, 996755. crossref

Ajmal, A., Danial, M., Zulfat, M., Numan, M., Zakir, S., Hayat, C., Alabbosh, K. F., Zaki, M. E., Ali, A., & Wei, D. (2024). In silico prediction of new inhibitors for kirsten rat sarcoma g12d cancer drug target using machine learning-based virtual screening, molecular docking, and molecular dynamic simulation approaches. *Pharmaceuticals*, *17*(5), 551. crossref

Arulselvan, P., Fard, M. T., Tan, W. S., Gothai, S., Fakurazi, S., Norhaizan, M. E., & Kumar, S. S. (2016). Role of antioxidants and natural products in inflammation. *Oxidative medicine and cellular longevity*, *2016*(1), 5276130. crossref

El-Moaty, Z. A., Aamer, H. A., Albishi, N. M., Al Abdulsalam, N. K., ALNasser, M. N., Augustyniak, M., El-Samad, L. M., & Aamer, N. A. (2026). The multifaceted effects of Melia azedarach leaf extract on Galleria mellonella: Enzymatic, histological and ultrastructural investigations. *Physiological Entomology*. crossref

Gomathi, D., Kalaiselvi, M., Ravikumar, G., Devaki, K., & Uma, C. (2015). GC-MS analysis of bioactive compounds from the whole plant ethanolic extract of Evolvulus alsinoides (L.) L. *Journal of food science and technology*, *52*(2), 1212-1217. crossref

Gomes, A., Fernandes, E., Lima, J. L., Mira, L., & Corvo, M. L. (2008). Molecular mechanisms of anti-inflammatory activity mediated by flavonoids. *Current medicinal chemistry*, *15*(16), 1586-1605. crossref

Haider, Z., Subhani, M. M., Farooq, M. A., Ishaq, M., Khalid, M., Khan, R. S. A., & Niazi, A. K. (2020). In Silico discovery of novel inhibitors against main protease (Mpro) of SARS-CoV-2 using pharmacophore and molecular docking based virtual screening from ZINC database. *Preprint*, *10*. crossref

Huang, Y., Gao, E., Liu, Q., Yuan, J., Wu, Y., Wang, W., & Rao, X. (2026). Anti-Hepatocarcinoma Activity and Mechanism of Isosendanin and Its Novel Structural Analogues Isolated from the Bark of Melia azedarach L.: In Vitro and In Vivo Studies. *Antioxidants*, *15*(5), 562. crossref

Jereva, D., Alov, P., Tsakovska, I., Angelova, M., Atanassova, V., Vassilev, P., Ikonomov, N., Atanassov, K., Pajeva, I., & Pencheva, T. (2022). Application of InterCriteria analysis to assess the performance of scoring functions in molecular docking software packages. *Mathematics*, *10*(15), 2549. crossref

Joshi, V., Kogularasu, S., Pant, P., Kung, H.-C., Wu, C.-H., Lu, M.-J., Duseja, M., Chitme, H., Sharma, N., & Bachhar, V. (2026). Green-Synthesized Fe3O4/Ag/ZnO Trimetallic Nanoparticles: Physicochemical Characterization, Antioxidant and Antidiabetic Activities, Histopathological and Serum Biochemical Evaluation, and Acute Toxicity Assessment. *Journal of Inorganic and Organometallic Polymers and Materials*, 1-18. crossref

Khan, M., Manzoor, Z., Rafiq, M., Munawar, S. H., Waqas, M. Y., Majeed, H., Ali Shah, S. Z., Hussain, R., Hussain, H. I., & Tahir, T. (2022). Phytochemical screening, anti-inflammatory, and antidiabetic activities of different extracts from Caralluma edulis plant. *Molecules*, *27*(16), 5346. crossref

Khan, M. F., Rawat, A. K., Khatoon, S., Hussain, M. K., Mishra, A., & Negi, D. S. (2018). In vitro and in vivo antidiabetic effect of extracts of Melia azedarach, Zanthoxylum alatum, and Tanacetum nubigenum. *Integrative Medicine Research*, *7*(2), 176-183. crossref

Kooti, W., Moradi, M., Ali-Akbari, S., Sharafi-Ahvazi, N., Asadi-Samani, M., & Ashtary-Larky, D. (2015). Therapeutic and pharmacological potential of Foeniculum vulgare Mill: a review. *Journal of HerbMed Pharmacology*, *4*(1), 1-9. reference

kumar Bargah, R. (2015). Preliminary test of phytochemical screening of crude ethanolic and aqueous extract of Moringa pterygosperma Gaertn. *Journal of Pharmacognosy and Phytochemistry*, *4*(1). reference

Kumari, S., Sangeetha, M., & Pavithra, R. (2016). A retrospective review on Indian traditional herbs and its biocompounds in diabetes. *Int. J. Pharm. Res*, *9*, 444-460. reference

M'rabet, Y., Rokbeni, N., Cluzet, S., Boulila, A., Richard, T., Krisa, S., Marzouki, L., Casabianca, H., & Hosni, K. (2017). Profiling of phenolic compounds and antioxidant activity of Melia azedarach L. leaves and fruits at two stages of maturity. *Industrial Crops and Products*, *107*, 232-243. crossref

Malar, T. J., Antonyswamy, J., Vijayaraghavan, P., Kim, Y. O., Al-Ghamdi, A. A., Elshikh, M. S., Hatamleh, A. A., Al-Dosary, M. A., Na, S. W., & Kim, H.-J. (2020). In-vitro phytochemical and pharmacological bio-efficacy studies on Azadirachta indica A. Juss and Melia azedarach Linn for anticancer activity. *Saudi journal of biological sciences*, *27*(2), 682-688. crossref

Mariadoss, A. V. A., Saravanakumar, K., Sathiyaseelan, A., Karthikkumar, V., & Wang, M.-H. (2022). Smart drug delivery of p-Coumaric acid loaded aptamer conjugated starch nanoparticles for effective triple-negative breast cancer therapy. *International journal of biological macromolecules*, *195*, 22-29. crossref

McCue, P. P., & Shetty, K. (2004). Inhibitory effects of rosmarinic acid extracts on porcine pancreatic amylase in vitro. *Asia Pacific Journal of Clinical Nutrition*, *13*(1). reference

Mechchate, H., Es-Safi, I., Louba, A., Alqahtani, A. S., Nasr, F. A., Noman, O. M., Farooq, M., Alharbi, M. S., Alqahtani, A., & Bari, A. (2021). In vitro alpha-amylase and alpha-glucosidase inhibitory activity and in vivo antidiabetic activity of Withania frutescens L. Foliar extract. *Molecules*, *26*(2), 293. crossref

Meena, G., Singh, B. P., Khatri, N., Yadav, U., & Pankaj, A. (2026). Pharmacological Properties of Melia Azedarach L.: A Review. *Int. J. Creative Res. Publ. Peer-Reviewed Journal Volume*, *1*(4). crossref

Molla, M. H. R., Aljahdali, M. O., Sumon, M. A. A., Asseri, A. H., Altayb, H. N., Islam, M. S., Alsaiari, A. A., Opo, F. D. M., Jahan, N., & Ahammad, F. (2023). Integrative ligand-based pharmacophore modeling, virtual screening, and molecular docking simulation approaches identified potential lead compounds against pancreatic cancer by targeting FAK1. *Pharmaceuticals*, *16*(1), 120. crossref

Nargund, R. R., Kulkarni, V. H., Habbu, P. V., AB, J., Goude, T., & Madagundi, S. D. (2018). Isolation, characterization of seconadry metabolites from the Melia azedarach Linn. Root and to evaluate their in vitro antidiabetic activity. *Journal of Pharmacognosy and Phytochemistry*, *7*(1), 2214-2220. reference

Naz, S., Farooq, U., Khan, S., Sarwar, R., Mabkhot, Y. N., Saeed, M., Alsayari, A., Muhsinah, A. B., & Ul-Haq, Z. (2021). Pharmacophore model-based virtual screening, docking, biological evaluation and molecular dynamics simulations for inhibitors discovery against α-tryptophan synthase from Mycobacterium tuberculosis. *Journal of Biomolecular Structure and Dynamics*, *39*(2), 610-620. crossref

Oyeleke, S. A., Ajayi, A. M., Umukoro, S., Aderibigbe, A., & Ademowo, O. G. (2018). Anti-inflammatory activity of Theobroma cacao L. stem bark ethanol extract and its fractions in experimental models. *Journal of ethnopharmacology*, *222*, 239-248. crossref

Padhi, S., Nayak, A. K., & Behera, A. (2020). Type II diabetes mellitus: a review on recent drug based therapeutics. *Biomedicine & Pharmacotherapy*, *131*, 110708. crossref

Rahman, A., Rehman, G., Shah, N., Hamayun, M., Ali, S., Ali, A., Shah, S. k., Khan, W., Shah, M. I. A., & Alrefaei, A. F. (2023). Biosynthesis and characterization of silver nanoparticles using Tribulus terrestris seeds: Revealed promising antidiabetic potentials. *Molecules*, *28*(10), 4203. crossref

Rauf, A., Rashid, U., Shah, Z. A., Rehman, G., Bashir, K., Jamil, J., Iftikhar, Rahman, A., Alsahammari, A., & Alharbi, M. (2023). Anti-inflammatory and anti-diabetic activity of ferruginan, a natural compound from olea ferruginea. *Processes*, *11*(2), 545. crossref

Rehman, G., Umar, M., Shah, N., Hamayun, M., Ali, A., Khan, W., Khan, A., Ahmad, S., Alrefaei, A. F., & Almutairi, M. H. (2023). Green synthesis and characterization of silver nanoparticles using Azadirachta indica seeds extract: in vitro and in vivo evaluation of anti-diabetic activity. *Pharmaceuticals*, *16*(12), 1677. crossref

Rehman, K., & Akash, M. S. H. (2017). Mechanism of generation of oxidative stress and pathophysiology of type 2 diabetes mellitus: how are they interlinked? *Journal of cellular biochemistry*, *118*(11), 3577-3585. crossref

Salehi, B., Ata, A., V. Anil Kumar, N., Sharopov, F., Ramirez-Alarcon, K., Ruiz-Ortega, A., Abdulmajid Ayatollahi, S., Valere Tsouh Fokou, P., Kobarfard, F., & Amiruddin Zakaria, Z. (2019). Antidiabetic potential of medicinal plants and their active components. *Biomolecules*, *9*(10), 551. crossref

Sanada, F., Taniyama, Y., Muratsu, J., Otsu, R., Shimizu, H., Rakugi, H., & Morishita, R. (2018). Source of chronic inflammation in aging. *Frontiers in cardiovascular medicine*, *5*, 12. crossref

Seifu, D., Gustafsson, L. E., Chawla, R., Genet, S., Debella, A., Holst, M., & Hellström, P. M. (2017). Antidiabetic and gastric emptying inhibitory effect of herbal Melia azedarach leaf extract in rodent models of diabetes type 2 mellitus. *Journal of experimental pharmacology*, 23-29. crossref

Sher, A., Sohail, A., Gul, A., Shan, A., Zman, K., Ali, A., & Rehman, G. (2026a). Green synthesis and characterization of silver nanoparticles using Asparagus officinalis and their anti-inflammatory and antioxidant activities: in silico, in vitro, and in vivo studies. *Journal of Drug Targeting*, 1-12. crossref

Sher, A., Sohail, A., Gul, A., Shan, A., Zman, K., Ali, A., & Rehman, G. (2026b). Green Synthesis and Characterization of Silver Nanoparticles Using Asparagus officinalis and their Anti-Inflammatory and Antioxidant Activities: In Silico, In Vitro, and In Vivo Studies. *Journal of Drug Targeting*(just-accepted), 1-16. crossref

Sher, A., Tsai, T.-C., Sohail, A., Alouffi, A., Almutairi, M. M., Wadood, A., Ajmal, A., Muhammad, W., Chen, C.-C., & Ali, A. (2025). Green synthesis of silver nanoparticles and characterization using Asparagus officinalis: Elucidation of Anti-diabetic potentials through In-Silico, In-Vitro, and In-Vivo Analyses. *Green Chemistry Letters and Reviews*, *18*(1), 2479589. crossref

Sher, A., Zaib, S., Sohail, A., Ahmad, A., Shan, A., Ali, A., & Rehman, G. (2026). Fungal-mediated synthesis of silver nanoparticles using Porostereum spadiceum and their antioxidant, anti-inflammatory, and antidiabetic activities. *The International Journal of Biochemistry & Cell Biology*, 106967. crossref

Shinkafi, T. S., Bello, L., Hassan, S. W., & Ali, S. (2015). An ethnobotanical survey of antidiabetic plants used by Hausa–Fulani tribes in Sokoto, Northwest Nigeria. *Journal of Ethnopharmacology*, *172*, 91-99. crossref

Singh, N., Baby, D., Rajguru, J. P., Patil, P. B., Thakkannavar, S. S., & Pujari, V. B. (2019). Inflammation and cancer. *Annals of African medicine*, *18*(3), 121-126. crossref

Sulimov, V. B., Kutov, D. C., Taschilova, A. S., Ilin, I. S., Tyrtyshnikov, E. E., & Sulimov, A. V. (2021). Docking paradigm in drug design. *Current Topics in Medicinal Chemistry*, *21*(6), 507-546. crossref

Taj, S., Ahmad, M., Alshammari, A., Alghamdi, A., & Ashfaq, U. A. (2022). Exploring the therapeutic potential of benzothiazine-pyrazole hybrid molecules against alpha-glucosidase: Pharmacological and molecular modelling based approach. *Saudi journal of biological sciences*, *29*(3), 1416-1421. crossref

Ukwuani, A., & Igbokwu, M. (2015). In vitro antidiabetic effect of Leptadenia hastata leaves fractions. *Biosciences Research in Today's World*, *1*(1), 40-46. crossref

Ullah, H., Nawaz, A., Rahim, F., Uddin, I., Hussain, A., Hayat, S., Zada, H., Khan, M. U., Khan, M. S., & Ajmal, A. (2023). Synthesis, in vitro β-glucuronidase inhibitory potential and molecular docking study of benzimidazole analogues. *Chemical Data Collections*, *44*, 100996. crossref

Zaharia, O. P., Strassburger, K., Strom, A., Bönhof, G. J., Karusheva, Y., Antoniou, S., Bódis, K., Markgraf, D. F., Burkart, V., & Müssig, K. (2019). Risk of diabetes-associated diseases in subgroups of patients with recent-onset diabetes: a 5-year follow-up study. *The lancet Diabetes & endocrinology*, *7*(9), 684-694. crossref